



Two-dimensional FTIR spectroscopic analysis of crystallization in cross-linked poly(ether ether ketone)

Abdul G. Al Lafi¹ · Ali Alzier¹ · Abdul W. Allaf¹

Received: 17 January 2019 / Accepted: 2 December 2019 / Published online: 1 January 2020
© Central Institute of Plastics Engineering & Technology 2020

Abstract

2D-COS-FTIR was used to locate the crystallization-sensitive bands of ion-irradiated poly(ether ether ketone). The band at 1310 cm^{-1} was the most sensitive band, and the area under this band changed linearly with the degree of crystallization which was obtained from differential scanning calorimetry. The deviation between experimentally determined and calculated degree of crystallization progressively increased at irradiation doses above 20 MGy for proton and helium-irradiated PEEK. This was attributed to different cross-linking mechanism on irradiation with the two different ions. 2D-COS-FTIR spectroscopy is a powerful tool for polymer characterization and helps in the quantitative analysis.

Keywords Cross-linking · Crystallization · Irradiation · IR spectra · Two-dimensional correlation spectroscopy

Introduction

Poly(ether ether ketone) (PEEK) is a high-temperature engineering polymer with high chemical, thermal, mechanical and radiation stabilities. These properties are highly associated with crystallinity and allow the polymer to be used in different applications, including structural materials in aerospace and nuclear reactors [1, 2] as well as in the development of polymer electrolyte membrane for fuel cells [3].

Irradiations have been utilized as mean to introduce cross-linking in the structure of PEEK [4–6] to improve its dimensional stability after chemical modification by sulfonation. The aim is being to produce materials with desirable combination of swelling and conductivity characteristics suitable for fuel cell application [3, 7].

PEEK crystallized with a simple two-phase morphology: amorphous and crystalline phase morphology, which makes it a suitable polymer for studying with Fourier-transform infrared (FTIR) spectroscopy [8]. Many researchers had carried out the investigation of PEEK crystallization by FTIR spectroscopy [9–12]. Such studies gave further insight to the molecular behavior and structural alteration within PEEK and PEEK systems including composite,

blends and cross-linked systems. Digital spectra subtraction and deconvolution are the available 1D techniques to identify crystalline bands and the components of overlap peaks [13]. However, the scope of this work was to apply the recent development in the field of FTIR analysis, in particular, two-dimensional correlation spectroscopy (2D-COS) for the analysis of FTIR spectra of cross-linked PEEK after crystallization. Since crystallization is related closely to the molecular structure, it is aimed in this study to provide evidence for the two different cross-linking types produced by different ion irradiations of PEEK.

2D-COS was first introduced to vibrational spectroscopy by Isao Noda [14] to simplify the complicated spectra, improve spectral resolution through the spreading of peaks over a second dimension and overcome the limitation encountered in 1D spectroscopy, i.e., the overlapped molecular events and weak signal-to-noise ratio (SNR). Since then, 2D-COS has been successfully applied for a wide range of spectroscopic analysis [15–17]. Another important feature of 2D-COS spectra is that they enable the determination of specific sequential order of spectral intensity changes that could be useful to study the mechanism of some processes [14, 18].

In this paper, FTIR spectra were measured for different helium-irradiated films of PEEK after they have been crystallized by the differential scanning calorimetry (DSC). 2D-COS analysis was applied to determine the bands and their relative sensitivity to change in molecular structure that

✉ Abdul G. Al Lafi
cscientific@aec.org.sy

¹ Department of Chemistry, Atomic Energy Commission, P.O. Box 6091, Damascus, Syrian Arab Republic

could be assigned to crystallization. 2D-COS analysis was also used as a tool to help in establishing the quantitative 1D analysis and increasing the accuracy of deconvolution process used to estimate the area under the predetermined bands by locating the bands and their overall change with external perturbation.

Materials and methods

Materials, sample preparation and DSC analysis

Amorphous PEEK in the form of 100- μm thick films with a density of 1260 kg m^{-3} was obtained from Goodfellow, UK. Helium ions irradiation was carried out using the University of Birmingham's Scanditronix MC40 Cyclotron operating at 25.6 MeV. The full experimental setups have been discussed in previous published articles [5].

The crystallized samples were prepared using a PerkinElmer differential scanning calorimeter, DSC-7 operating under argon atmosphere at a flow rate of $20 \text{ cm}^3 \text{ min}^{-1}$ and heating and cooling rates of $20 \text{ }^\circ\text{C min}^{-1}$. The apparatus was set to run a program consisting of three steps to ensure the same thermal history for each PEEK sample.

The first heating scan was performed from 50 to $360 \text{ }^\circ\text{C}$, after cooling; a second heating scan to $360 \text{ }^\circ\text{C}$ was performed followed by cooling scan from $360 \text{ }^\circ\text{C}$ to the start temperature. The enthalpy and temperature calibrations were carried out using ultrapure metal standards: indium (melting point, m.pt.: 429.78 K , $\Delta H_f = 29.2 \text{ J g}^{-1}$), tin (m.pt.: 505.06 K) and lead (m.pt.: 600.65 K). The degree of crystallinity was determined from the heat absorbed during melting in the second heating scan and the heat of crystallization for the totally crystalline PEEK, which was taken to be 122.5 J g^{-1} , using the equation [19]:

$$\%X_w = \frac{\Delta H}{\Delta H_m^0} \times 100. \quad (1)$$

Infrared spectroscopy and 2D correlation analysis

A Thermo Scientific Nicolet 6700 FTIR spectrometer (Madison, USA), JASCO-ATR accessory and a DTGS detector were used to record IR spectra of ion-irradiated PEEK samples after crystallization. All IR spectra were measured from 400 to 4000 cm^{-1} at a resolution of 2 cm^{-1} with a total of 200 scans. A separate background spectrum was subtracted in each data acquisition.

All spectra were baseline corrected, smoothed with a Savitzky–Golay smoothing function of two polynomials and 13 points and finally normalized to the same thickness based on the 1600 cm^{-1} band as discussed in previous articles

[20, 21]. 2D correlation analysis was performed using the algorithm developed by Noda [14, 22], and the calculation and visualization of the 2D spectra (synchronous and asynchronous) were carried out using the 2DShige version 1.3 software (Shigeaki Morita, Kwansai-Gakuin University, 2004–2005). The reference spectrum was taken as the spectrum of the sample with maximum absorbed dose, i.e., at the lower crystallization degree. Two types of correlation spectra are obtained from a generalized 2D correlation analysis. The synchronous spectrum provides information about the similarity between responses of the FTIR bands to a perturbation, degree of crystallization in this work. The asynchronous correlation spectrum, on the other hand, locates variations in spectral intensities that are not synchronously correlated [14]. In the 2D correlation spectra, the positive (shown in white or red areas) and negative (shown in gray or blue areas) cross-peaks in both synchronous and asynchronous spectra were interpreted by means of Noda's rule [22].

X-ray diffraction

Powder X-ray diffraction, XRD, patterns of PEEK samples were recorded using a transmission diffractometer (STADI-P STOE, Darmstadt, Germany), with $\text{CuK}\alpha$ radiation ($\lambda = 1.54060 \text{ \AA}$) and a germanium monochromator operated at 50 kV and 30 mA .

Results and discussion

General remarks

DSC, see Fig. 1a, was used to confirm that the changes observed in FTIR were due to crystallization, the samples were thermally stable, and no post-irradiation effects were taking place. The weight degrees of crystallinity were determined from Eq. (1), and the results are depicted in Fig. 1b. As expected, the degree of crystallization decreased with the progressive increase in irradiation dose.

The FTIR spectrum of amorphous PEEK is well documented and the structural alterations that occur on morphology change (crystallization) or on chemical modification (sulfonation) as well as the reactions that accompany ion irradiation have been all reported and discussed based on the FTIR spectra [13, 21].

Figure 2 shows the FTIR spectra of helium-irradiated PEEK samples after they have been crystallized in the DSC. Some spectral features are clearly seen such as those in the regions 1600 – 1660 cm^{-1} (shift of the carbonyl band), 1250 – 1450 cm^{-1} (shift and appearance of new bands) and 800 – 900 cm^{-1} (splitting).

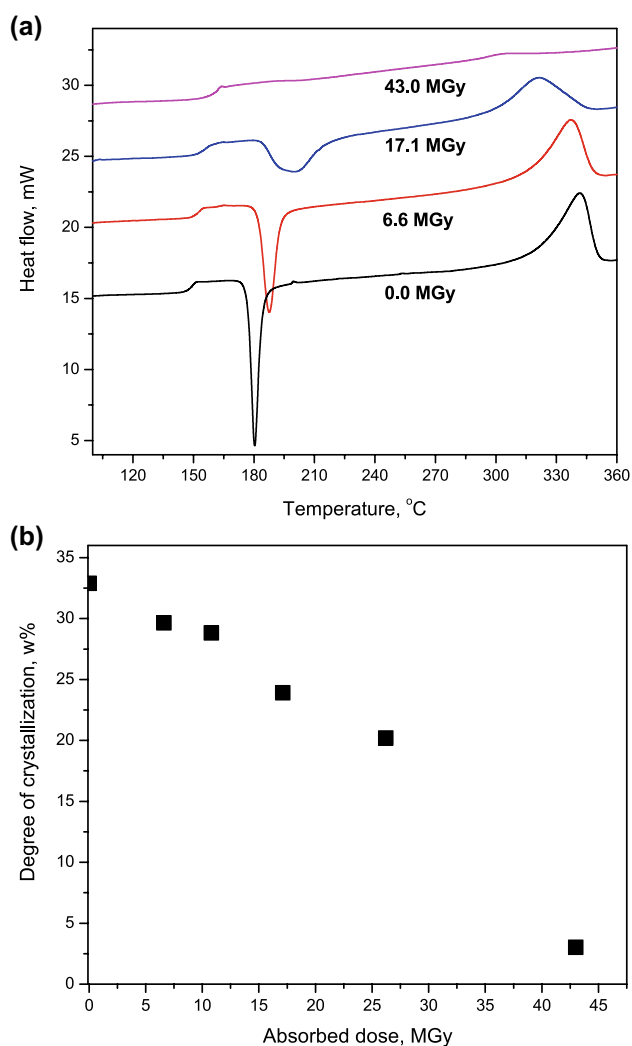


Fig. 1 a DSC profiles on the first heating scan of helium-irradiated PEEK, b the calculated degree of crystallization as a function of absorbed dose

2D-COS-FTIR analysis

Although there are many available techniques including digital spectra subtraction, derivative and deconvolution [23] to analyze the FTIR spectra, 2D-COS has been used in the present work to extract subtle changes and to identify the real crystalline bands. In comparison with 1D techniques, 2D-COS treats the whole spectral data and extracts the bands that respond selectively to the external perturbation and also enable the sequence of spectral peaks emergence to be determined [17, 24]. Only the two regions from 1250 to 1325 cm^{-1} and from 900 to 1000 cm^{-1} were considered due to their quantitative relation to crystallization in uncross-linked PEEK. In particular, the changes include the absorbance or area ratios of the bands at 1305/1280 cm^{-1} , 970/952 cm^{-1} and 947 cm^{-1} [9, 11, 25].

The region 1325–1250 cm^{-1}

Figure 3a shows the synchronous spectrum of helium-irradiated PEEK after crystallization. There were auto-peaks at 1310, 1295, 1285, 1275 and 1255 cm^{-1} , positive cross-peaks that correlated the bands at (1310, 1285), (1295, 1255) and (1270, 1255) cm^{-1} and negative cross-peaks that correlated the bands at (1310, 1295), (1310, 1270), (1310, 1255) and (1285, 1255) cm^{-1} . This suggested that the bands at 1295, 1255 and 1270 cm^{-1} change in the same direction but in the opposite direction to the bands at 1310 and 1285 cm^{-1} that increased in intensity with increasing crystallization degree.

The corresponding asynchronous spectrum is shown in Fig. 3b and reveals the presence of positive cross-peaks that correlated the bands at (1310, 1295), (1310, 1273), (1285, 1270) and (1310, 1255) cm^{-1} . There were also negative cross-peaks that correlated the bands at (1320, 1310), (1295, 1285) and (1320, 1285) cm^{-1} . The signs of the cross-peaks suggested the earlier occurrence of the intensity decrease at 1295, 1270 and 1255 cm^{-1} over the intensity increase at 1310 and 1285 cm^{-1} .

Assuming that cross-linked PEEK crystallized with a simple two-phase morphology similar to PEEK, and based on the 2D analysis, the two bands at 1310 and 1285 cm^{-1} are attributed to crystalline phase and the other bands at 1295, 1255 and 1270 cm^{-1} are attributed to amorphous phase. The two bands at 1295 and 1275 cm^{-1} have been shown to be sensitive to changes in the molecular structure of PEEK [13]. Upon crystallization, they shifted to new positions at 1310 and 1285 cm^{-1} which are assigned to the bending motion of the C–C(=O)–C and the asymmetric stretching of the diphenyl ether groups, respectively [20].

The region 1000–900 cm^{-1}

Figure 4a shows the synchronous spectrum in this region. There were auto-peaks at 965, 950, 940, 930, 925 and 918 cm^{-1} , negative cross-peaks that correlated the bands at (940, 930), (930, 925), (925, 918), (975, 930), (975, 918), (998, 925), (965, 925) and (950, 925) cm^{-1} , and positive cross-peaks that correlated the bands at (930, 918), (975, 940), (998, 965), (998, 950), (998, 930), (998, 918), (965, 950), (965, 930), (965, 918), (950, 930) and (950, 918) cm^{-1} . This suggested that the bands at 998, 965, 950, 930 and 918 cm^{-1} change in the same direction but in the opposite direction to the bands at 940, 925 and 975 cm^{-1} that decreased in intensity with increasing crystallization degree. This implied that the bands at 998, 965, 950, 930 and 918 cm^{-1} are related to crystallization.

The corresponding asynchronous spectrum of Fig. 4b shows the main asynchronous cross-peaks. There were positive cross-peaks that correlated the bands at (930, 918), (950, 918), (965, 918), (965, 900), (995, 925), (918, 900),

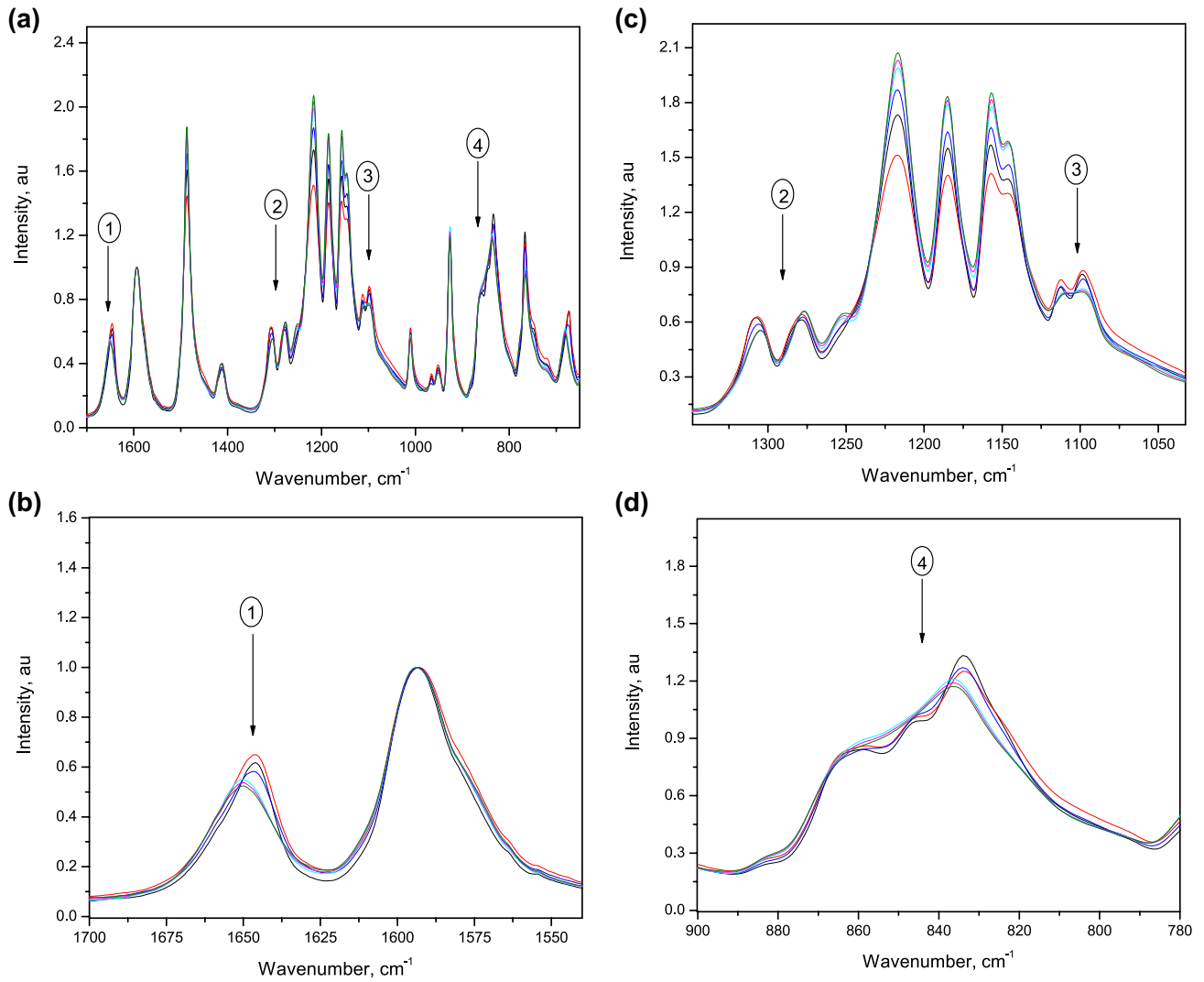


Fig. 2 IR spectra of ion-irradiated PEEK after crystallization in the DSC

Fig. 3 **a** Synchronous and **b** asynchronous 2D correlation spectra of irradiated and melt-crystallized PEEK in the region 1325–1250 cm^{-1}

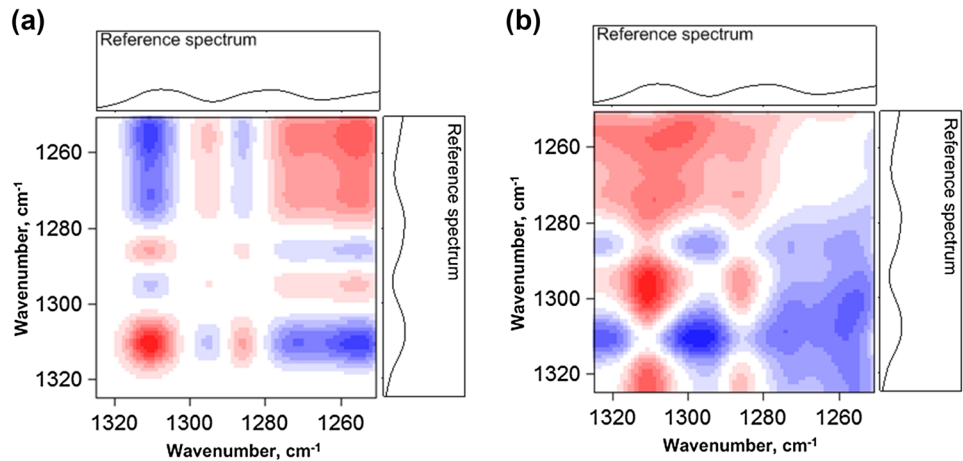
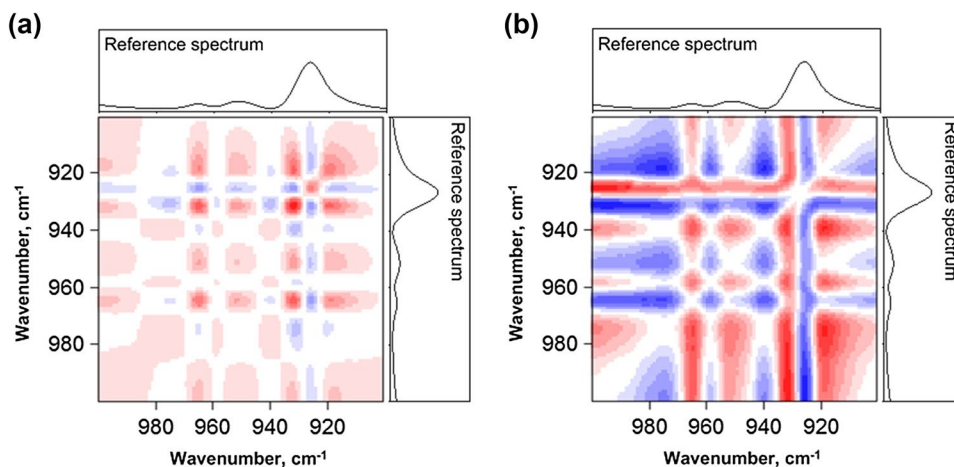


Fig. 4 **a** Synchronous and **b** asynchronous 2D correlation spectra of irradiated and melt-crystallized PEEK in the region 1000–900 cm^{-1}



(950, 940), (965, 940), (995, 940), (995, 960) and (995, 975) cm^{-1} . There were also negative cross-peaks that correlated the bands at (925, 918), (940, 918), (965, 918), (975, 918), (940, 930), (965, 930), (975, 932), (995, 930), (965, 950) and (975, 965) cm^{-1} . The signs of cross-peaks indicated that the intensity decrease in the bands at 915, 950, 930 and 995 cm^{-1} occurred after the intensity increase in the bands at 925, 975, and 940 cm^{-1} .

Based on the 2D analysis, the bands at 995, 965, 950, 930 and 918 cm^{-1} are attributed to crystalline phase and the other bands at 975, 940 and 925 cm^{-1} are attributed to amorphous phase. The 950 cm^{-1} band increased in the present study with increasing crystallization degree, while the band at 965 cm^{-1} was less sensitive to crystallization. This confirmed that the 950 cm^{-1} band was due to the formation of ordered structure and crystallization. On the other hand, the band at 925 cm^{-1} , which is assigned to diphenylketone stretching, was split into two components at 930 and 918 cm^{-1} . They are assigned to cross-linked structure produced by helium irradiation and to the attachment of polar groups on the aromatic rings [20, 26, 27].

The sequential order

The order of crystalline bands change could be obtained from the signs of cross-peaks from both synchronous and asynchronous spectra by analyzing the different regions in the FTIR spectra according to Noda rule [14, 22]. The following order of band change was deduced: 1310 \rightarrow 1285 \rightarrow 930 \rightarrow 950 \rightarrow 965 \rightarrow 918. This order of band change indicated that the two bands at 1310 and 1285 cm^{-1} were the most sensitive to crystallization as they change before other bands, while the two bands at 965 and 918 cm^{-1} were the least sensitive. This was consistent with the literatures, as it has been shown that the 965 cm^{-1} band is very weakly sensitive to the degree of crystallinity above 15% [11]. It has also been reported [25] in the case of non-cross-linked

PEEK that the band at $1310 \pm 5 \text{ cm}^{-1}$ was more sensitive to crystalline conformers than the band at $1285 \pm 5 \text{ cm}^{-1}$. It could be concluded that 2D-COS is a suitable technique to derive the FTIR sensitive crystallization bands.

Degree of crystallization from FTIR analysis

A deconvolution algorithm (OMNIC software) was applied to resolve the overlap in the two bands located in the region from 1340 to 1260 cm^{-1} , as depicted in Fig. 5.

Following the procedure outlined in the literatures, [9, 11] the area under each crystallized band was calculated and correlated with the degree of crystallization, which was obtained from the DSC analysis of the corresponding samples. The results obtained are plotted in Fig. 6a, b. Both examined ratios 1310/1285 and 965/950 were not a linear function of crystallization over all crystallization range

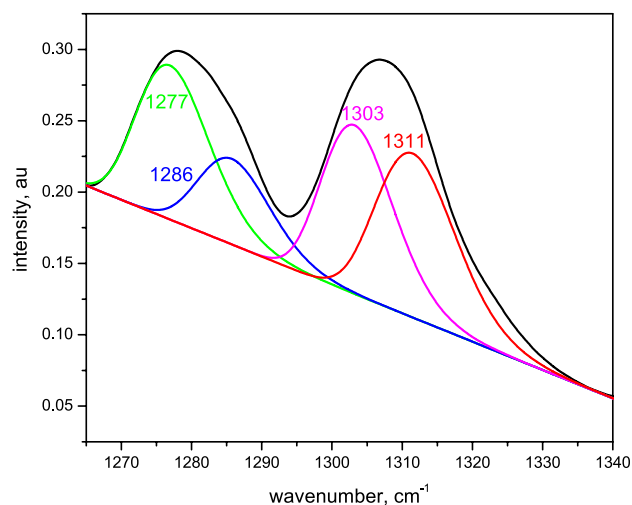


Fig. 5 Deconvolution of the bands in the region 1260–1340 cm^{-1} for crystallized ion-irradiated PEEK sample

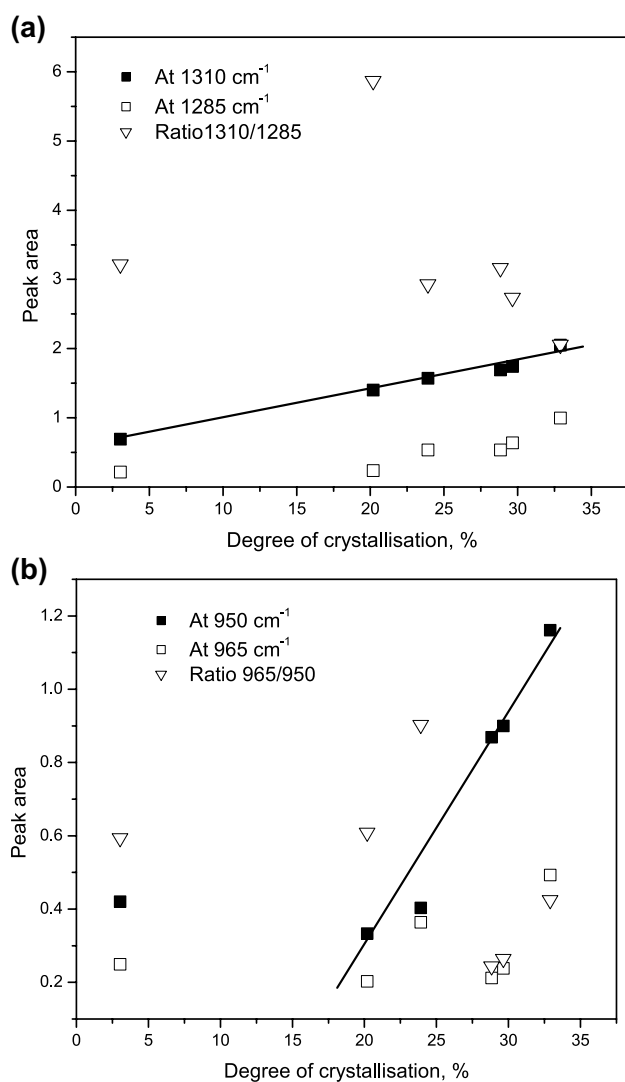


Fig. 6 Absorbance peak area against crystallinity for ion-irradiated PEEK samples. **a** In the region 1285–1310 cm^{-1} , **b** in the region 950–965 cm^{-1}

studied. However, the ratio 1310/1285 was linear above 15% crystallization and was more representative for crystallization than the ratio at 965/950. This could be due to similar ratios of the extinction coefficient of the amorphous and the crystalline regions resulted by the introduction of cross-linking in the amorphous region [25]. Another possibility to account for the nonlinear behavior of the ratios is that some FTIR bands consisted of not only amorphous and crystalline components. It has been reported that amorphous PEEK contains an intermediate phase called rigid phase [28]. It seems likely that this rigid phase was enhanced by the introduction of cross-linking which improves the backing efficiency of the chains [6]. The shifts observed in the most FTIR band in the cross-linked PEEK support the later conclusion.

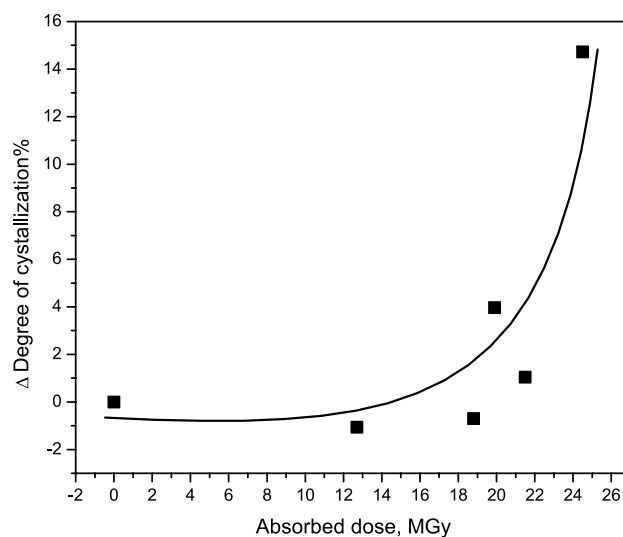


Fig. 7 Difference between measured DSC crystallization and the one calculated from Eq. (2)

On the other hand, a linear relation was only obtained with the area under the band at 1310 cm^{-1} with a correlation coefficient of 0.989, Fig. 6a. This suggests that X_w of cross-linked PEEK could be estimated from the following relation,

$$\%X_w = \frac{A_{1310} - (0.55 \pm 0.08)}{(0.042 \pm 0.003)} \times 100 \quad (2)$$

where A_{1310} is the area under the band at 1310 cm^{-1} after normalizing the spectrum based on the 1600 cm^{-1} band.

Estimation the crystallization degrees of proton-irradiated PEEK

The degree of crystallization of proton-irradiated PEEK samples were calculated from the corresponding FTIR spectra by the use of Eq. (2) and correlated with the DSC results. The difference between the measured values of crystallization and the calculated ones, Δ , was plotted in Fig. 7 as a function of the absorbed dose. As can be seen, the differences below 20 MGy were within experimental error, but they progressively increased at higher doses.

The band at 1310 cm^{-1} is assigned to the bending motion of the carbonyl bridge C–C(=O)–C [20], and it is directly related to the formation of zigzag structure upon crystallization of PEEK. Figure 8 shows typical X-ray diffraction patterns in the region of $2\theta = 10^\circ$ – 36° for PEEK and proton-irradiated PEEK after being melt-crystallized. The main reflections (110), (111), (200) and (211) could be clearly identified, and the crystalline structures were reserved after cross-linking [8, 29, 30].

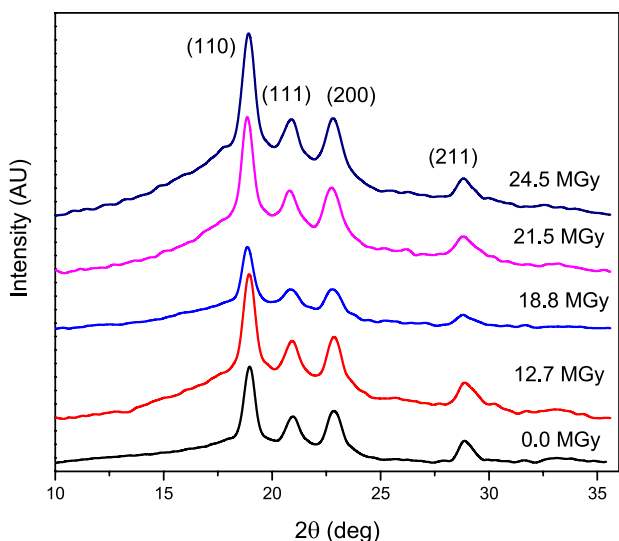
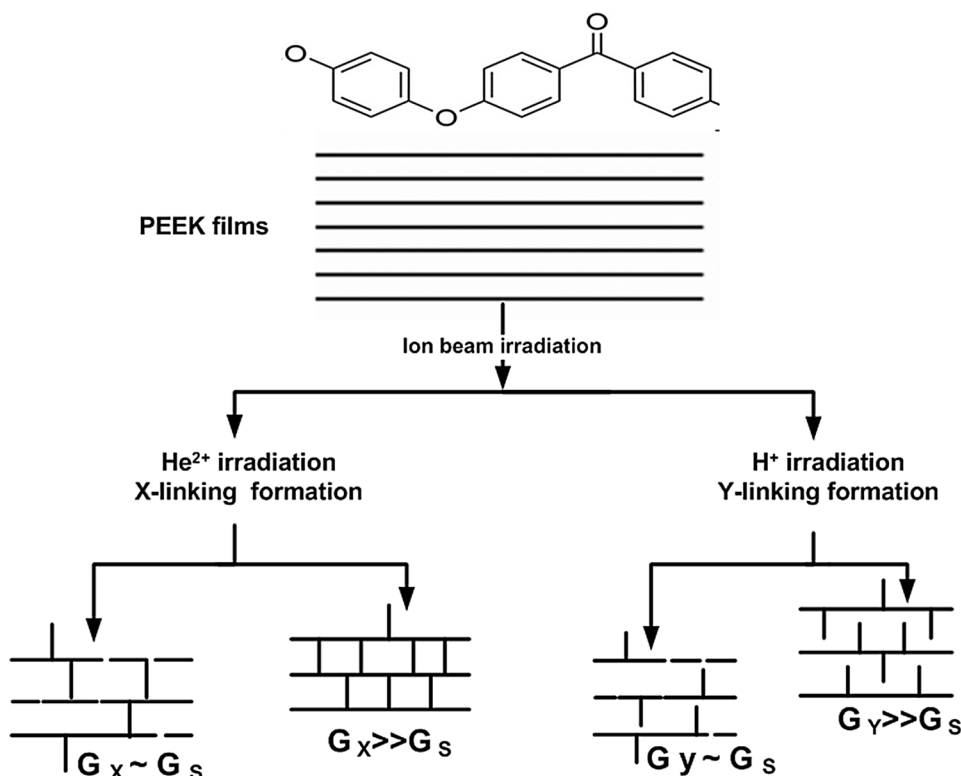


Fig. 8 X-ray diffraction patterns of PEEK and proton-irradiated PEEK samples after melt crystallization in the DSC

Therefore, the difference could be attributed to the change in cross-linking type with increasing absorbed dose as it has been reported recently [31]. The possible cross-linking types that could be produced on ion irradiation are shown in Fig. 9 based on the differences on the G values of the corresponding ion [32]. The G_x values of x -linking, G_y , and y -linking, G_y , increased with increasing irradiation

Fig. 9 Possible cross-linked structure of ion-irradiated PEEK



dose, and the G value of chain scission reaction, G_s , of H^+ is much higher than that of He^{2+} [5].

Conclusion

Attenuated total reflection Fourier-transform infrared (ATR-FTIR) and two-dimensional correlation (2D-COS) spectroscopies were applied to identify the structural alteration related to crystallization of He^{2+} ion-irradiated PEEK films. The 2D analysis was used to deduce the spectrum of crystallized ion-irradiated PEEK, determine the sequential order of crystalline band changes and identify the suitable bands that could be used to determine the degree of crystallization. The FTIR bands of cross-linked PEEK could be treated as arising from overlapping components due to different molecular structures in amorphous, cross-linked and crystalline regions. It is valuable to perform 2D analysis prior to the use of a specific band to perform quantitative analysis and estimating the degree of crystallization.

Acknowledgements The author thanks Prof. James N. Hay for useful discussion and Prof. David J. Parker for allowing the use of irradiation facility. Thanks are also due to Prof. I. Othman the General Director of the AEC of Syria and Prof. Z. Ajji the Head of Chemistry Department for their encouragements.

References

1. El-Sayed AH, Sasuga T, Seguchi T (1992) Irradiation effects on aromatic polymers: 3. Changes in thermal properties by gamma irradiation. *Polymer* 33(14):2911–2914
2. Sasuga T, Kudoh H (2000) Ion irradiation effects on thermal and mechanical properties of poly(ether-ether-ketone) PEEK. *Polymer* 41(1):185–194
3. Chen J et al (2007) Double crosslinked polyetheretherketone-based polymer electrolyte membranes prepared by radiation and thermal crosslinking techniques. *Polymer* 48(20):6002–6009
4. Macková A et al (2005) Degradation of PET, PEEK and PI induced by irradiation with 150 keV Ar⁺ and 1.76 MeV He⁺ ions. *Nuclear Instrum Methods Phys Res B* 240(1–2):245–249
5. Al-Lafi AG (2012) The effects of ion irradiation on the dielectric properties of poly(ether ether ketone). *Polym Bull* 68(9):2269–2283
6. Al-Lafi AG (2014) Structural development in ion-irradiated poly(ether ether ketone) as studied by dielectric relaxation spectroscopy. *J Appl Polym Sci* 131(6):2593–2601
7. Al-Lafi AG, Hay JN (2015) State of the water in crosslinked sulfonated poly(ether ether ketone). Two-dimensional differential scanning calorimetry correlation mapping. *Thermochim Acta* 612:63–69
8. Blundell DJ, Osborn BN (1983) The morphology of poly(aryl-ether-ether-ketone). *Polymer* 24:953–958
9. Chalmers JM, Gaskin WF, Mackenzie MW (1984) Crystallinity in poly(aryl-ether-ketone) plaques studied by multiple internal reflection spectroscopy. *Polym Bull* 11(5):433–435
10. Nguyen HX, Ishida H (1986) Molecular analysis of the crystallization behaviour of poly(aryl-ether-ether-ketone). *J Polym Sci Part B Polym Phys* 24(5):1079–1091
11. Jonas A, Legras R, Issi J-P (1991) Differential scanning calorimetry and infra-red crystallinity determinations of poly(aryl ether ether ketone). *Polymer* 32(18):3364–3370
12. Damman P et al (1994) Crystallinity of poly(aryl ether ether ketone) by vibrational spectroscopy. *Macromolecules* 27(6):1582–1587
13. Nguyen HX, Ishida H (1986) Molecular analysis of the melting behaviour of poly(aryl-ether-ether-ketone). *Polymer* 27(9):1400–1405
14. Noda I (1993) Generalized two-dimensional correlation method applicable to infrared. *Raman Other Types Spectrosc Appl Spectrosc* 47(9):1329–1336
15. Al-Lafi AG, Hay JN (2017) The isothermal crystallization of poly(ether ether ketone) by two-dimensional differential scanning calorimetry correlation mapping. *J Appl Polym Sci* 134(4):44378
16. Al-Lafi AG, Ajji Z (2017) Radiation grafting of acrylic acid and N-vinyl imidazole onto polyethylene films for lead ion removal: a two-dimensional correlation infrared spectroscopy investigation. *J Appl Polym Sci* 134(19):44781
17. Park Y, Noda I, Jung YM (2016) Novel developments and applications of two-dimensional correlation spectroscopy. *J Mol Struct* 1124:11–28
18. Noda I (2010) Two-dimensional correlation spectroscopy—biannual survey 2007–2009. *J Mol Struct* 974(1–3):3–24
19. Kong Y, Hay JN (2003) The enthalpy of fusion and degree of crystallinity of polymers as measured by DSC. *Eur Polym J* 39(8):1721–1727
20. Al-Lafi AG (2014) FTIR spectroscopic analysis of ion irradiated poly(ether ether ketone). *Polym Degrad Stab* 105:122–133
21. Al-Lafi AG (2015) The sulfonation of poly(ether ether ketone) as investigated by two-dimensional FTIR correlation spectroscopy. *J Appl Polym Sci* 132(2):41242
22. Noda I, Ozaki Y (2004) Two-dimensional correlation spectroscopy: applications in vibrational and optical spectroscopy. Wiley, Chichester
23. Stuart BH (2004) Infrared spectroscopy: fundamentals and applications. Wiley, Chichester
24. Choi HC et al (2010) Two-dimensional heterospectral correlation analysis of X-ray photoelectron spectra and Infrared spectra for spin-coated films of biodegradable poly(3-hydroxybutyrate-co-3-hydroxyhexanoate) copolymers. *J Phys Chem B* 114:10979–10985
25. Voice AM, Bower DI, Ward IM (1993) Molecular orientation in uniaxially drawn poly(aryl ether ether ketone): 2. Infra-red spectroscopic study. *Polymer* 34(6):1164–1173
26. Socrates G (2001) Infrared and Raman characteristic group frequencies tables and charts, 3rd edn. Wiley, London
27. Silverstein RM, Webster FX, Kiemle DJ (2005) Spectrometric identification of organic compounds, 7th edn. Wiley, New York
28. Goodwin AA, Simon GP (1996) Glass transition behaviour of poly(ether ether ketone)/poly(ether imide) blends. *Polymer* 37:991–995
29. Hay JN, Langford JJ, Lloyd JR (1989) Variation in unit cell parameters of aromatic polymers with crystallization temperature. *Polymer* 30(3):489–493
30. Kong Y, Hay JN (2003) The enthalpy of fusion and degree of crystallinity of polymers as measured by DSC. *Eur Polym J* 39:1721–1727
31. Al-Lafi AG (2018) Application of 2D correlation methods to the analysis of XPS spectra of ion irradiated poly(ether ether ketone). *J Polym Res* 25:105
32. Cumpson PJ et al (2013) X-ray enhanced sputter rates in argon cluster ion sputter-depth profiling of polymers. *J Vac Sci Technol B Nanotechnol Microelectron Mater Process Meas Phenom*. <https://doi.org/10.1116/1.4793284>

Publisher's Note Springer Nature remains neutral with regard to jurisdictional claims in published maps and institutional affiliations.